



Effects of Molecular Structure and Aggregated Structure on Photoluminescence Properties of Liquid-crystalline Gold(I) Complexes with Various Aromatic Rings

Osama Younis, Yuki Rokusha, Nana Sugimoto, Kaori Fujisawa, Shigeyuki Yamada & Osamu Tsutsumi

To cite this article: Osama Younis, Yuki Rokusha, Nana Sugimoto, Kaori Fujisawa, Shigeyuki Yamada & Osamu Tsutsumi (2015) Effects of Molecular Structure and Aggregated Structure on Photoluminescence Properties of Liquid-crystalline Gold(I) Complexes with Various Aromatic Rings, Molecular Crystals and Liquid Crystals, 617:1, 21-31, DOI: 10.1080/15421406.2015.1075367

To link to this article: <http://dx.doi.org/10.1080/15421406.2015.1075367>



Published online: 07 Oct 2015.



Submit your article to this journal [↗](#)



Article views: 15



View related articles [↗](#)



View Crossmark data [↗](#)

Effects of Molecular Structure and Aggregated Structure on Photoluminescence Properties of Liquid-crystalline Gold(I) Complexes with Various Aromatic Rings

OSAMA YOUNIS, YUKI ROKUSHA, NANA SUGIMOTO,
KAORI FUJISAWA[†], SHIGEYUKI YAMADA,
AND OSAMU TSUTSUMI*

Department of Applied Chemistry, College of Life Sciences, Ritsumeikan University, Kusatsu, Japan

Rod-like gold(I) complexes with phenyl, biphenyl, or naphthyl rings in a mesogenic core were synthesized by complexation of ethynyl-substituted aromatic derivatives with (tetrahydrothiophene)AuCl, followed by ligand exchange with alkyl isocyanide, to investigate the effects of molecular and molecular-aggregated structures on their liquid-crystalline (LC) behavior and photoluminescence properties. The gold complexes exhibited enantiotropic liquid crystallinity. Introduction of multi-ring systems into the mesogenic core effectively expanded the LC temperature range. A comparison of the photoluminescence properties in the crystalline phase showed that the molecular-aggregated structure plays a crucial role in the luminescence of these gold complexes.

Keywords gold(I) complex; aggregation-induced emission; aurophilic interaction; liquid crystal; photoluminescence

Introduction

Strongly photoluminescent molecules in condensed phases have attracted attention as promising candidates for materials for light-emitting devices [1]. However, most organic molecules are not emissive in the condensed phase because of the concentration-quenching effect or aggregation-caused quenching, even if they show strong photoluminescence in dilute solutions. Recent advances in the study of condensed-phase photoluminescent materials have led to the successful development of a new class of materials with enhanced emission intensities in the condensed phase, known as aggregation-induced emission (AIE) materials [2]. Among AIE materials, organic complexes containing gold atoms have attracted considerable interest in the fields of photonics and electronics because they exhibit strong emissions in condensed phases as a result of inter- or intra-molecular interactions

[†]Present Address: Department of Organic Chemistry, University of Geneva

*Address correspondence to Osamu Tsutsumi, Department of Applied Chemistry, College of Life Sciences, Ritsumeikan University, 1-1-1 Nojihigashi, Kusatsu 525-8577, Japan. E-mail: tsutsumi@sk.ritsumei.ac.jp

Color versions of one or more of the figures in the article can be found online at www.tandfonline.com/gmcl.

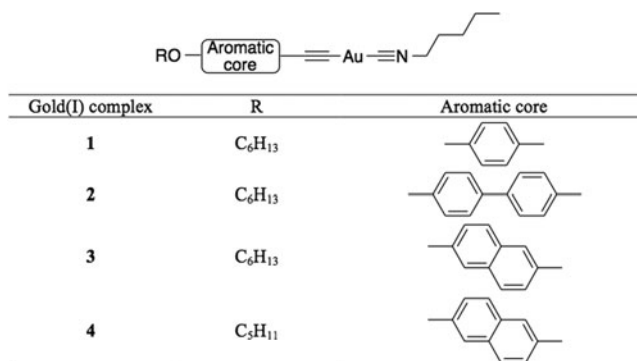


Figure 1. Structures of gold(I) complexes used in this study.

between gold atoms (aurophilic interactions); however, individual non-aggregated gold complexes are non-emissive in dilute solutions [3–7].

Our research focuses on the development of liquid-crystalline (LC) gold(I) complexes. We have found that gold(I) complexes with LC properties exhibit strong photoluminescence in condensed phases [4]; for example, gold complexes with a phenyl, biphenyl, or naphthyl group in a mesogenic core have an enantiotropic nematic (N) phase, and the temperature range of the N phase depends strongly on the structure of the mesogenic core. In addition, these complexes emit strong blue or green photoluminescence, depending on both the molecular and molecular-aggregated structures, in the crystalline phases. To control the LC properties and luminescence properties, the relationship between these properties and the molecular and/or molecular-aggregated structures need to be clarified. In this study, we synthesized gold complexes with different π -electron systems in the mesogenic core and flexible chains, and compared their LC behaviors and luminescence properties.

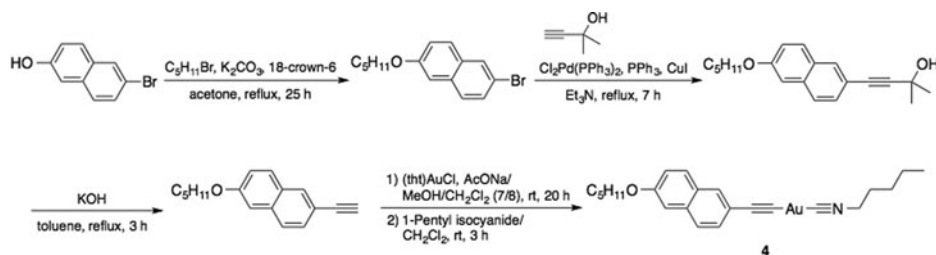
Experimental

Materials

Figure 1 shows the structures of the gold(I) complexes synthesized in this study. The syntheses of complexes **1–3** have been reported previously [4]. The new complex **4** was synthesized by alkylation of (tht)AuCl (tht = tetrahydrothiophene), followed by ligand exchange with 1-pentyl isocyanide (Scheme 1). All solvents and reagents used were reagent grade and commercially available, and were used without further purification unless otherwise stated. ¹H nuclear magnetic resonance (NMR) spectra were recorded in CDCl₃ at 400 MHz, using a JEOL ECS-400 spectrometer. Chemical shifts are reported in parts per million (ppm), using the residual proton in the NMR solvent as an internal reference.

Synthesis of 6-Bromo-2-(pentyloxy)naphthalene

6-Bromo-2-naphthol (2.7 g, 12 mmol), potassium carbonate (2.8 g, 20 mmol), 1-bromopentane (1.5 g, 10 mmol), and 18-crown-6 (0.13 g, 0.51 mmol) were added to acetone (15 mL), and the resulting mixture was refluxed for 24 h. The solid in the reaction mixture was filtered off, and the filtrate was evaporated under reduced pressure. The residue was



Scheme 1. Synthetic route to complex 4.

dissolved in CH_2Cl_2 , and then sequentially washed with water, 1.5 M aqueous sodium hydroxide solution, water, and brine. The organic layer was dried over anhydrous Na_2SO_4 , filtered, and concentrated *in vacuo* using a rotary evaporator. The title compound was obtained in 50% yield (1.5 g, 6.0 mmol). ^1H NMR (400 MHz, CDCl_3 , δ): 7.90 (d, $J = 2.3$ Hz, 1H, 5-*H* in naphthalene), 7.64 (d, $J = 9.1$ Hz, 1H, 4-*H* in naphthalene), 7.58 (d, $J = 8.6$ Hz, 1H, 8-*H* in naphthalene), 7.48 (dd, $J = 8.6$ and 1.8 Hz, 1H, 7-*H* in naphthalene), 7.16 (dd, $J = 8.9$ and 2.5 Hz, 1H, 3-*H* in naphthalene), 7.08 (d, $J = 2.3$ Hz, 1H, 1-*H* in naphthalene), 4.06 (t, $J = 6.6$ Hz, 2H, OCH_2), 1.85 (quin, $J = 7.0$ Hz, 2H, OCH_2CH_2), 1.53–1.36 (m, 4H, $(\text{CH}_2)_2$), 0.95 (t, $J = 7.2$ Hz, 3H, CH_3).

Synthesis of 4-[2-(Pentyloxy)naphthalene-6-yl]-3-butyne-2-ol

6-Bromo-2-(pentyloxy)naphthalene (1.4 g, 4.9 mmol), 2-methyl-3-butyne-2-ol (1.4 g, 17 mmol), triphenylphosphine (48 mg, 0.18 mmol), bis(triphenylphosphine)palladium dichloride (112 mg, 0.16 mmol), and copper iodide (38 mg, 0.20 mmol) were dissolved in triethylamine (20 mL), and the resulting mixture was refluxed for 13 h under argon. After stirring for 13 h, the precipitate formed in the reaction mixture was removed by filtration, and the filtrate was concentrated using a rotary evaporator. The resultant mixture was dissolved in CH_2Cl_2 , and then washed sequentially with water, saturated aqueous NH_4Cl solution, water, and brine. The organic layer was dried over anhydrous Na_2SO_4 , filtered, and concentrated *in vacuo*. The crude product was purified using silica-gel column chromatography (eluent: CH_2Cl_2), giving the title compound in 64% yield (0.96 g, 3.1 mmol). ^1H NMR (400 MHz, CDCl_3 , δ): 7.85 (s, 1H, 5-*H* in naphthalene), 7.67 (d, $J = 8.6$ Hz, 1H, 4-*H* in naphthalene), 7.63 (d, $J = 8.6$ Hz, 1H, 8-*H* in naphthalene), 7.41 (dd, $J = 8.6$ and 1.8 Hz, 1H, 7-*H* in naphthalene), 7.14 (dd, $J = 8.8$ and 2.5 Hz, 1H, 3-*H* in naphthalene), 7.08 (d, $J = 2.3$ Hz, 1H, 1-*H* in naphthalene), 4.06 (t, $J = 6.6$ Hz, 2H, OCH_2), 2.05 (s, 1H, OH), 1.85 (quin, $J = 7.0$ Hz, 2H, OCH_2CH_2), 1.65 (s, 6H, $\text{C}(\text{CH}_3)_2\text{OH}$), 1.53–1.36 (m, 4H, $\text{O}(\text{CH}_2)_2(\text{CH}_2)_2$), 0.95 (t, $J = 7.2$ Hz, 3H, $\text{O}(\text{CH}_2)_5\text{CH}_3$).

Synthesis of 6-Ethynyl-2-(pentyloxy)naphthalene

The prepared propargyl alcohol derivative (0.96 g, 3.1 mmol) and potassium hydroxide (0.73 g, 13 mmol) were dissolved in toluene (40 mL), and the mixture was refluxed for 3 h. The solid in the reaction mixture was filtered off, and the filtrate was sequentially washed with saturated aqueous NH_4Cl solution, water, and brine. The organic layer was dried over anhydrous Na_2SO_4 , filtered, and concentrated under reduced pressure. The crude product was purified using silica-gel column chromatography (eluent: *n*-hexane/ $\text{AcOEt} = 4/1$), giving the title compound in 69% yield (0.53 g, 2.2 mmol). ^1H NMR (400 MHz,

CDCl_3 , δ): 7.94 (s, 1H, 5-*H* in naphthalene), 7.69 (d, $J = 9.1$ Hz, 1H, 4-*H* in naphthalene), 7.65 (d, $J = 8.6$ Hz, 1H, 8-*H* in naphthalene), 7.48 (dd, $J = 8.4$ and 1.6 Hz, 1H, 7-*H* in naphthalene), 7.16 (dd, $J = 9.1$ and 2.3 Hz, 1H, 3-*H* in naphthalene), 7.09 (d, $J = 2.7$ Hz, 1H, 1-*H* in naphthalene), 4.07 (t, $J = 6.6$ Hz, 2H, OCH_2), 3.10 (s, 1H, $-\text{C}\equiv\text{CH}$), 1.85 (quin, $J = 7.0$ Hz, 2H, OCH_2CH_2), 1.53–1.36 (m, 4H, $\text{O}(\text{CH}_2)_2(\text{CH}_2)_2$), 0.95 (t, $J = 7.2$ Hz, 3H, CH_3).

Synthesis of Gold Complex 4

A solution of sodium acetate (0.21 g, 2.5 mmol) in $\text{CH}_2\text{Cl}_2/\text{MeOH}$ (6.0 mL/2.0 mL) was added to a solution of 6-ethynyl-2-(pentyloxy)naphthalene (0.13 g, 0.54 mmol) and (tht)AuCl (0.19 g, 0.62 mmol) in a mixed $\text{CH}_2\text{Cl}_2/\text{MeOH}$ (1.0 mL/6.0 mL) solvent under an argon atmosphere, followed by stirring at room temperature for 22 h. The precipitate formed in the reaction mixture was collected by filtration and sequentially washed with MeOH, water, MeOH, and CH_2Cl_2 . The yellow solid obtained was suspended in CH_2Cl_2 (10 mL), and 1-pentyl isocyanide (82 μL , 0.65 mmol) was added to the resultant suspension. The mixture was stirred at room temperature for 3 h, and then passed through Celite, followed by removal of the solvent *in vacuo*. The resultant yellow solid was purified by recrystallization from CH_2Cl_2 /heptane, providing pale-yellow needle-like crystals of **4** in 62% yield (0.18 g, 0.34 mmol). mp 107°C. ^1H NMR (400 MHz, CDCl_3 , δ): 7.78 (s, 1H, 5-*H* in naphthalene), 7.63 (d, $J = 8.6$ Hz, 1H, 4-*H* in naphthalene), 7.59 (d, $J = 8.6$ Hz, 1H, 8-*H* in naphthalene), 7.39 (dd, $J = 8.6$ and 1.8 Hz, 1H, 7-*H* in naphthalene), 7.12–7.08 (m, 2H, 1,3-*H* in naphthalene), 4.05 (t, $J = 6.6$ Hz, 2H, OCH_2), 3.63 (t, $J = 6.8$ Hz, 2H, NCH_2), 1.87–1.77 (m, 4H, OCH_2CH_2 , NCH_2CH_2), 1.51–1.33 (m, 8H, $\text{OCH}_2\text{CH}_2(\text{CH}_2)_2$, $\text{NCH}_2\text{CH}_2(\text{CH}_2)_2$), 0.94 (t, $J = 7.0$ Hz, 6H, $\text{O}(\text{CH}_2)_5\text{CH}_3$, $\text{N}(\text{CH}_2)_4\text{CH}_3$).

X-Ray Crystallography

A single crystal of gold complex **4** was obtained by slow evaporation from CH_2Cl_2 /hexane (1/1), and then mounted on a glass fiber. The omega scanning technique was used to collect the reflection data, using a Bruker D8 goniometer with graphite-monochromatized Mo $K\alpha$ radiation ($\lambda = 0.71075$ Å). The measurements were performed at room temperature (296 K). The initial structure of the unit cell was determined by a direct method using APEX2. The structural model was refined by a full-matrix least-squares method using XSELL V6.3.1. All calculations were performed using SHELXL programs. The crystal data of gold complex **4** in Table 1 have been indexed and are included in the Cambridge Crystallographic Center (CCDC) database with the following reference number: CCDC 1043338. The indexed database contains additional supplementary crystallographic data for this paper and may be accessed without charge at <http://www.ccdc.cam.ac.uk/conts/retrieving.html>. The CCDC may be contacted by mail at 12 Union Road, Cambridge CB2 1EZ, U.K., by fax at (44) 1223-336-033, or by e-mail at deposit@ccdc.cam.ac.uk.

Phase-Transition Behavior

The LC behaviors of the gold complexes were investigated by polarizing optical microscopy (POM) using an Olympus BX51 equipped with a hot stage (Instec HCS302 hot stage and mK1000 controller). Thermogravimetric analysis (TGA) and differential thermal analysis were performed, using a DTG-60AH unit (Shimadzu), at heating rate of 1.0°C/min, to assess the thermal stabilities of the gold complexes. The thermodynamic properties of the

Table 1. Crystallographic data for gold(I) complexes 1–4

Gold(I) complex	1	2	3	4
Empirical formula	C ₂₀ H ₂₈ AuNO	C ₂₆ H ₃₂ AuNO	C ₂₄ H ₃₀ AuNO	C ₂₃ H ₂₈ AuNO
Formula weight	495.4	571.49	545.20	531.44
Temperature (K)	296	93 (2)	296	296
Color, habit	Colorless, plate	Colorless, plate	Pale yellow, needle	Pale yellow, needle
Crystal size (mm)	0.44 × 0.18 × 0.04	0.15 × 0.15 × 0.05	0.50 × 0.20 × 0.05	0.15 × 0.15 × 0.05
Crystal system	Triclinic	Monoclinic	Monoclinic	Triclinic
$R[F^2 > 2\sigma(F^2)]$	0.045	0.0439	0.0493	0.0455
$wR(F^2)$	0.125	0.0976	0.1082	0.0953
Space group	$P\bar{1}$	$P2_1/n$	$P2_1/c$	$P\bar{1}$
Z	2	8	4	2
a (Å)	7.3596 (8)	9.6606(13)	15.0415(8)	8.8000(13)
b (Å)	9.8116 (2)	14.538(2)	16.3652(9)	9.5780(14)
c (Å)	13.9641 (2)	33.229(5)	9.2192(5)	14.120(2)
α (degree)	89.373 (7)	–	–	107.288(3)
β (degree)	88.527 (9)	93.054(2)	97.1360(17)	98.101(3)
γ (degree)	83.285 (6)	–	–	102.352(3)
V (Å ³)	1001.06(16)	2251.8(2)	1083.1(3)	108.1(3)

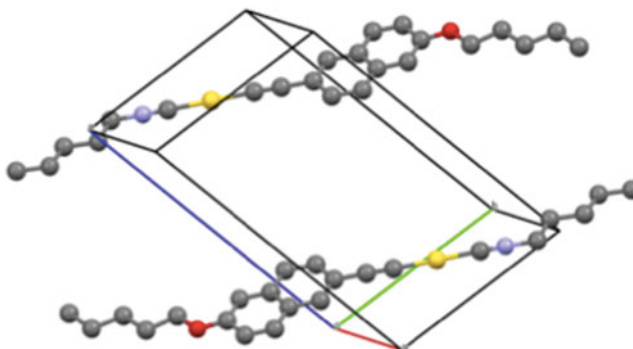


Figure 2. Crystal structure of complex **4**; hydrogen atoms are omitted for clarity.

LC gold complexes were determined using differential scanning calorimetry (DSC; SII X-DSC7000) at heating and cooling rates of 5.0°C/min. At least three scans were performed to check the reproducibility.

Photophysical Properties

Ultraviolet/visible (UV-vis) absorption spectra were recorded using a JASCO V-500 absorption spectrophotometer. Steady-state photoluminescence spectra were obtained using a Hitachi F-7000 fluorescence spectrophotometer.

Results and Discussion

Synthesis and Crystal Structure of Gold Complex 4

The novel gold(I) complex **4** was synthesized as shown in Scheme 1. First, an alkynyl ligand was prepared by Williamson etherification of 6-bromo-2-naphthol with 1-bromopentane, followed by a Sonogashira cross-coupling reaction with 2-methyl-3-butyne-2-ol, and then elimination of acetone (see Experimental section). Reaction of the alkynyl ligand with (tht)AuCl in the presence of sodium acetate, followed by addition of 1-pentyl isocyanide, gave the desired gold complex **4** in 62% yield as pale-yellow needle-like crystals, which were characterized using ^1H NMR spectroscopy and single-crystal X-ray crystallography.

The crystal structure of complex **4** is shown in Figure 2, and the crystallographic data for gold complexes **1–4** are summarized in Table 1. The presence of aurophilic interactions in complexes **1–4** was determined based on the interatomic distances between the nearest-neighbor gold atoms; the values are listed in Table 2.

Gold complex **4**, with a naphthalene core bearing a pentyloxy chain, crystallized in the *P*-1 triclinic space group, with two formula units in the unit cell (Figure 2). Although the difference between the molecular structures of complexes **3** and **4** was slight, distinct crystal packing structures were observed. The distances between neighboring gold atoms in **2–4** were longer than 3.9 Å (Table 2), whereas the sum of the van der Waals radii of two gold atoms is 3.8 Å [5], suggesting that intermolecular Au...Au (aurophilic) interactions do not occur in these gold complexes. In contrast, our previous study showed that gold complex **1**, with a phenyl ring, had aurophilic interactions in the crystal phase (Au...Au distance: 3.55 Å) [4c].

Table 2. Distances between neighboring gold atoms and presence of aurophilic interactions

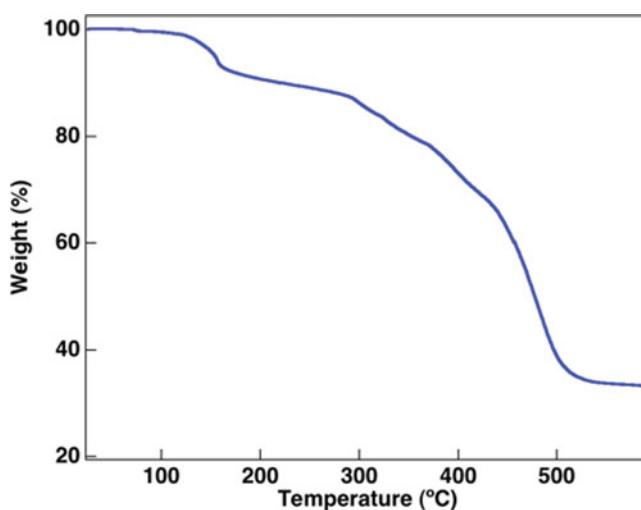
	Distance between neighboring gold atoms (Å)	Aurophilic interaction
1	3.55	Yes
2	3.95	No
3	4.60	No
4	4.78	No

Thermal Stability of Gold(I) Complex 4

The thermal stability of gold complex **4** was investigated using TGA. The results are shown in Figure 3. We estimated the thermal decomposition temperature of **4** to be 154°C; this was the temperature at which 5% weight loss occurred. The thermal decomposition temperature of **4** was similar to those of gold complexes **1–3**, determined in our previous studies: 148, 165, and 147°C for **1**, **2**, and **3** respectively [4]. On the basis of these results, we concluded that the thermal stabilities of LC gold complexes with 1-pentyl isocyanide ligands are not affected by the aromatic ring structure in the mesogenic core. We have also reported previously that LC gold complexes with phenyl isocyanide ligands have high thermal stabilities [4b]. The thermal decomposition temperatures of all the gold complexes with 1-pentyl isocyanide ligands were close to the boiling point of 1-pentyl isocyanide (137–138°C), therefore we deduced that cleavage of the coordination bond between the gold atom and the 1-pentyl isocyanide ligand occurs at the thermal decomposition temperature.

LC Behavior of Gold(I) Complexes

We examined the LC behavior of gold complex **4**; the POM image obtained is shown in Figure 4. All the gold complexes used in this study exhibited an enantiotropic N LC phase.

**Figure 3.** TGA thermogram of complex **4**; heating rate = 1.0°C/min.

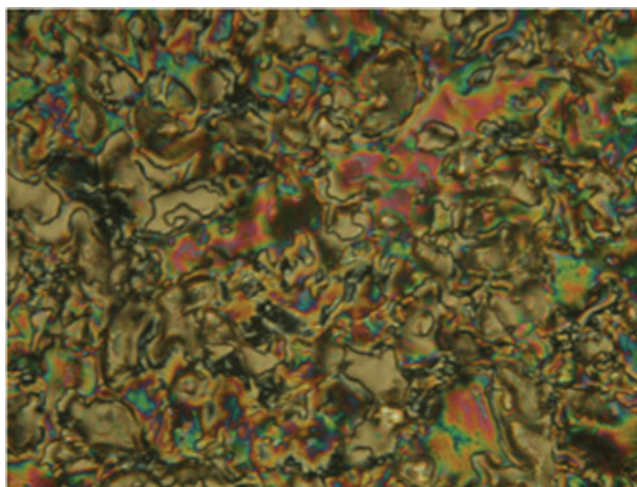


Figure 4. POM image of **4** at 120°C in first cooling scan.

The LC-phase sequences and phase-transition temperatures, determined using DSC, are summarized in Table 3.

Gold complex **1**, with a phenyl ring, displayed the N phase in a very narrow temperature range (approximately 4°C). However, a significant increase in the temperature range of the LC phase was induced by incorporation of a multi-ring system into the mesogenic core. The biphenyl ring is highly symmetric, which causes both the melting point and the clearing temperature to increase. However, because the naphthalene ring decreased the symmetry of the mesogen, the clearing temperature and melting point decreased. Complexes **3** and **4** therefore exhibited the N phase over wider temperature ranges than **1**, and at lower temperatures than **2**.

A comparison of the LC behaviors of complexes **3** and **4** showed that the length of the alkyl chain was also important for the stability of the LC phase. Complex **4**, which had a shorter alkyl chain, showed the N phase at a much lower temperature over a much wider

Table 3. Phase-transition behaviors of gold(I) complexes **1–4**

Complex	Phase-transition temperature ^{a,b} (°C)	
1	Heating	Cr 89 N 93 I
	Cooling	Cr 70 N 94 I
2	Heating	Cr 146 N 165 Dec.
	Cooling	Cr 117 N 165 Dec.
3	Heating	Cr 124 N 131 I
	Cooling	Cr 82 N 130 I
4	Heating	Cr 107 N 126 I
	Cooling	Cr 99 N 124 I

^aAbbreviations: Cr, crystalline; N, nematic; I, isotropic; Dec., thermal decomposition.

^bData refer to DSC scan. Phase-transition temperatures were determined as peak onset.

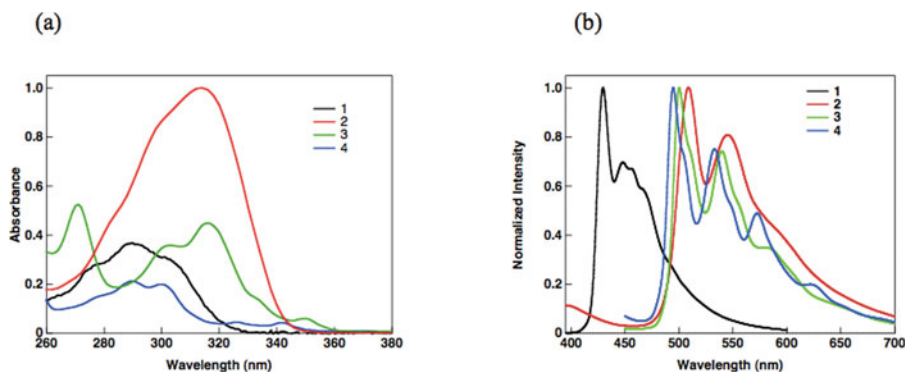


Figure 5. (a) Absorption spectra of gold(I) complexes **1–4** in CH₂Cl₂: black, **1** (2.7×10^{-5} mol/L); red, **2** (1.0×10^{-5} mol/L); green, **3** (1.0×10^{-5} mol/L); and blue, **4** (1.0×10^{-5} mol/L). (b) Photoluminescence spectra of LC gold complexes in crystalline phase at room temperature: black, **1** ($\lambda_{\text{ex}} = 340$ nm); red, **2** ($\lambda_{\text{ex}} = 360$ nm); green, **3** ($\lambda_{\text{ex}} = 364$ nm); and blue, **4** ($\lambda_{\text{ex}} = 364$ nm).

temperature range. Tuning of both the structure of the π -ring system in the mesogenic core and the length of the flexible chain is important in achieving the desired LC behavior.

Photophysical Properties of LC Gold(I) Complexes

The photophysical properties of the gold complexes were examined (Figure 5). As can be seen in Figure 5a, solutions of the LC gold complexes in CH₂Cl₂ absorbed light in the UV region, but were completely transparent in the visible range; these are favorable properties for their practical use in light-emitting materials. Figure 5b shows the crystalline-phase photoluminescence spectra of LC complexes **1–4**. The emission maxima appeared at 430, 510, 505, and 495 nm for **1**, **2**, **3**, and **4**, respectively. Moreover, the shapes of the spectra and the photoluminescence wavelengths of **2–4**, with multi-ring systems, were similar to each other, but those of complex **1**, with a single-ring system, differed from those of the others.

The photoluminescence quantum yields of the LC gold complexes in the crystalline phase were also estimated, and the results are summarized in Table 4. It has been reported that the quantum yield of LC gold complex **1** was 50% [4c]. However, complexes **2–4**, with multi-ring systems, had much lower quantum yields, less than 10%. These results indicate that the photoluminescence properties of the complex with a single aromatic ring system are different from those of the complexes with multi-ring systems in the

Table 4. Photoluminescence quantum yields of gold complexes in crystal

Gold(I) complex	Quantum yield ^a
1	0.50
2	0.08
3	0.04
4	0.09

^aDetermined at room temperature in air.

mesogenic structure. Differences among the crystal structures of the complexes could explain the difference between the properties of complex **1** and those of the others. As shown by the data in Table 2, aurophilic interactions were observed only in complex **1** (the closest interatomic distance between gold atoms was 3.55 Å), whereas no aurophilic interactions were observed in complexes **2–4**, with multi-ring systems. No significant differences among the photoluminescence properties of gold complexes **2–4** were observed, although they had different aromatic ring systems and/or flexible side chains of different lengths. It can therefore be concluded that molecular aggregates play a crucial role in the photoluminescence of gold complexes, but the structure of the π -electron system and the alkyl side chain in the molecule do not affect the photoluminescence in the present system.

Conclusion

In this work, the effects of the molecular structures and aggregated structures of gold(I) complexes on LC behavior and photoluminescence properties were investigated. The gold complexes exhibited enantiotropic LC behavior, and a wider temperature range of the LC phase was achieved by expansion of aromatic–ring system of the mesogenic cores. Furthermore, photoluminescence was observed in the crystalline phase, and the luminescence properties depended not only on the molecular structure, π -electron system, and alkyl chain, but also on the aggregated structure of the complex. Further investigations by our group are currently ongoing, to enhance the LC and photoluminescence behaviors of new gold complexes for applications as light-emitting materials.

Acknowledgments

This work was partly supported by the MEXT-Supported Program for the Strategic Research Foundation at Private Universities, 2012–2016, JSPS KAKENHI (Grant No. 24550217), and JST A-STEP (AS231Z04286D). This research was also supported by the Kyoto Advanced Nanotechnology Network (Nara Institute of Science and Technology), and by the Cooperative Research Program of Network Joint Research Center for Materials and Devices (Tokyo Institute of Technology).

References

- [1] Shinar, J., & Savateev, V. (2004). *Organic Light-emitting Devices: A Survey*, Chapter 1, Springer: New York, 1.
- [2] (a) Zhao, Z., Lam, J. W. Y., & Tang, B. Z. (2013). *Soft Mater.*, 9, 4564. (b) Zhao, Z., Lam, J. W. Y., & Tang, B. Z. (2012). *J. Mater. Chem.*, 22, 23726. (c) Hong, Y., Lam, J. W. Y., & Tang, B. Z. (2011). *Chem. Soc. Rev.*, 40, 5361. (d) Hong, Y., Lam, J. W. Y., & Tang, B. Z. (2009). *Chem. Commun.*, 4332. (e) An, B.-K., Kwon, S.-K., Jung, S.-D., & Park, S. Y. (2002). *J. Am. Chem. Soc.*, 124, 14410.
- [3] (a) Gavara, R., Llorca, J., Lima, J. C., & Rodriguez, L. (2013). *Chem. Commun.*, 49, 72. (b) Baron, M., Tubaro, C., Biffis, A., Basato, M., Graiff, C., Poater, A., Cavallo, L., Armaroli, N., & Accorsi, G. (2012). *Inorg. Chem.*, 51, 1778. (c) Rawashdeh-Omary, M. A., López-de-Luzuriaga, J. M., Rashdan, M. D., Elbjeirami, O., Monge, M., Rodríguez-Castillo, M., & Laguna, A. (2009). *J. Am. Chem. Soc.*, 131, 3824. (d) Schmidbaur, H., Cronje, S., Djordjevic, B., & Schuster, O. (2005). *Chem. Phys.*, 311, 151.
- [4] (a) Sugimoto, N., Tamai, S., Fujisawa, K., & Tsutsumi, O. (2014). *Mol. Cryst. Liq. Cryst.*, 601, 97. (b) Fujisawa, K., Okuda, Y., Izumi, Y., Nagamatsu, A., Rokusha, Y., Sadaike, Y., & Tsutsumi, O. (2014). *J. Mater. Chem. C*, 2, 3549. (c) Fujisawa, K., Kawakami, N., Onishi, Y., Izumi, Y.,

- Tamai, S., Sugimoto, N., & Tsutsumi, O. (2013). *J. Mater. Chem. C*, *1*, 5359. (d) Fujisawa, K., Izumi, Y., Nagamatsu, A., Uno, K., & Tsutsumi, O. (2012). *Mol. Cryst. Liq. Cryst.*, *563*, 50. (e) Rokusha, Y., Sugimoto, N., Yamada, S., & Tsutsumi, O. (2014). *Proc. SPIE*, *9182*, 918206, DOI: 10.1117/12.2060334.
- [5] Schmidbaur, H. (2000). *Gold Bull.*, *33*, 3.
- [6] Tiekink, E. R. T., & Kang, J.-G. (2009). *Coord. Chem. Rev.*, *253*, 1627.
- [7] Koshevoy, I. O., Sminova, E. S., Hauka, M., Laguna, A., Chueca, J. C., Pakkanen, T. A. Tunik, S. P., Ospino, I., & Crespo, O. (2011). *Dalton Trans.*, *40*, 7412.